HHS Public Access

Author manuscript

Sci Transl Med. Author manuscript; available in PMC 2015 May 05.

Published in final edited form as:

Sci Transl Med. 2014 November 5; 6(261): 261ra151. doi:10.1126/scitranslmed.3010162.

Regional delivery of mesothelin-targeted CAR T cell therapy generates potent and long-lasting CD4-dependent tumor immunity

Prasad S. Adusumilli[1,2], **Leonid Cherkassky**[1,2,†], **Jonathan Villena-Vargas**[1,2,†], **Christos Colovos**[1,2], **Elliot Servais**[1,2], **Jason Plotkin**[1], **David R. Jones**[2], and **Michel Sadelain**[1]

[1]Center for Cell Engineering, Memorial Sloan Kettering Cancer Center, New York, NY

[2]Thoracic Service, Department of Surgery, Memorial Sloan Kettering Cancer Center, New York, NY

Abstract

Translating the recent success of chimeric antigen receptor (CAR) T cell therapy for hematological malignancies to solid tumors will necessitate overcoming several obstacles, including inefficient T cell tumor infiltration and insufficient functional persistence. Taking advantage of an orthotopic model that faithfully mimics human pleural malignancy, we evaluated two routes of administration of mesothelin-targeted T cells using the M28z CAR. We found that intra-pleurally administered CAR T cells vastly out-performed systemically infused T cells, requiring 30-fold fewer M28z T cells to induce long-term complete remissions. Following intrapleural T cell administration, prompt *in vivo* antigen-induced T cell activation allowed robust CAR T cell expansion and effector differentiation, resulting in enhanced anti-tumor efficacy and functional T cell persistence for 200 days. Regional T cell administration also promoted efficient elimination of extrathoracic tumor sites. This therapeutic efficacy was dependent on early CD4+ T cell activation associated with a higher intra-tumoral CD4/CD8 cell ratios and CD28-dependent CD4+ T cell-mediated cytotoxicity. In contrast, intravenously delivered CAR T cells, even when accumulated at equivalent numbers in the pleural tumor, did not achieve comparable activation, tumor eradication or persistence. The remarkable ability of intrapleurally administered T cells to circulate and persist supports the concept of delivering optimal CAR T cell therapy through "regional distribution centers." Based on these results, we are opening a phase I clinical trial to

Corresponding Authors: Prasad S. Adusumilli, MD, FACS, FCCP, Center for Cell Engineering, Department of Surgery, Thoracic Service, adusumip@mskcc.org, Michel Sadelain MD, PhD, Center for Cell Engineering, Immunology Program, Sloan Kettering Institute, sadelaim@mskcc.org, Memorial Sloan Kettering Cancer Center, NY 10065, 1275 York Ave., New York, NY 10065, Tel: 212-639-8093/212-639-6190, Fax: 646-422-2340/917-432-2340.

[†]These authors contributed equally to the work and should be considered as second authors

Author Contributions: ***Conception and design:*** PSA, MS
Development of methodology: PSA, MS
Acquisition of data: PSA, LC, JV, CC, ES, JP
Analysis and interpretation of data: PSA, LC, JV, CC, ES, DRJ, MS
Writing, review and revision of the manuscript: PSA, LC, JV, CC, ES, DRJ, MS
Administrative, technical, or material support: PSA, DRJ, MS
Study supervision: PSA, MS

Competing Interests: The authors declare no conflicts of interest.

evaluate the safety of intrapleural administration of mesothelin-targeted CAR T cells in patients with primary or secondary pleural malignancies.

Introduction

Pleural malignancies, both primary (malignant pleural mesothelioma, MPM) and metastatic (from lung and breast cancers), affect more than 150,000 patients per year in the U.S. alone (1). MPM is a regionally aggressive disease with limited treatment options (2). We and others have reported on the better prognosis of having higher levels of tumor-infiltrating lymphocytes in MPM (3-6), suggesting that T cell-based immunotherapy may be beneficial to patients with MPM (7).

Targeted immunotherapies utilizing chimeric antigen receptors (CARs) to redirect and reprogram patient T cells have recently shown encouraging results in some B cell malignancies, especially acute lymphoblastic leukemia and non-Hodgkin lymphoma (8-11). CARs are synthetic receptors that retarget T cells to tumor surface antigens (12, 13). The advent of second generation CARs, which combine activating and costimulatory signaling domains, has enabled the design of potent T cells that can mediate complete responses in patients with chemo refractory CD19+ malignancies(8-11). The therapeutic potential of CAR therapies against solid cancers remains unknown. One critical aspect of devising a CAR therapy for any solid tumor is the identification of a valid target antigen. Mesothelin (MSLN) is a cell surface molecule associated with regional invasion, a characteristic of MPM where it is overexpressed in more than 90% of epithelioid MPM (14). In our clinicopathological studies systematically evaluating MSLN expression and intensity, we found strong to intermediate MSLN expression in 69% of lung adenocarcinoma (n=1209) (15), 36% of triple-negative breast cancer (n=355) and 46% of esophageal adenocarcinoma (n=125) (16). MSLN expression was consistently associated with tumor aggressiveness and decreased survival (14-16). Collectively, these observations support targeting MSLN in MPM and other solid cancers (7, 17-19).

Mesothelin-targeted CARs have previously shown activity in a subcutaneous model of mesothelioma (20-22). Targeted T cell therapies have however not been studied in orthotopic models. To this end, we established a clinically relevant MPM mouse model that recapitulates characteristic features of the human disease (14, 23, 24). The established pleural tumors encase lung and mediastinal structures with regional invasion, show extensive lymphangiogenesis and develop mediastinal lymph node metastases. In this model, we not only addressed whether CAR T cells could eradicate tumor but studied two potential routes of T cell administration: the conventional systemic intravenous and regional intra-pleural administration. We hypothesized that systemic delivery may be superior owing to better infiltration of diffuse pleural disease, mediastinal lymph nodes and occasional metastatic sites, which we could model. To our surprise, we found that regional, i.e. intra-pleural T cell administration, was vastly superior, not only against pleural disease but also against disseminated tumor sites. This observation prompted us to investigate the basis for such therapeutic efficacy.

Here, we report the therapeutic potential of regional CAR T-cell therapy for solid tumors and underscore the importance of early-antigen activation of CD4+ CAR T cells to achieve enhanced antitumor efficacy. Furthermore, our findings, which demonstrate the clear benefit of regional therapy in a clinically relevant disease model, are immediately translatable for the treatment of MPM and metastatic pleural tumors.

Results

Mz- and M28z-transduced T cells specifically respond to MSLN+ target cells

We constructed two CARs incorporating a human MSLN-specific scFv(25) and either CD3ζ or CD28/CD3ζ signaling domains (Mz and M28z, Fig. 1A). The P28z CAR, specific for prostate-specific membrane antigen (PSMA)(26), served as a negative control for alloreactivity and xenoreactivity. Both CD4+ and CD8+ human peripheral blood T lymphocytes were effectively transduced using the SFG gamma-retroviral vector (60-75% transduction, Fig. S1A). MSLN-transduced MSTO-211H (MSLN+) and PSMA-transduced EL-4 mouse lymphoma cells (MSLN-) cells provided MSLN positive and negative targets used for *in vitro* experiments (Fig. S1B). Mz- and M28z-transduced T cells demonstrated similar MSLN-specific lysis *in vitro*. (Fig. 1B). P28z CAR T cells did not lyse MSTO MSLN+ and mesothelin-targeted CARs did not lyse EL4 PSMA+. As expected for second generation CARs,(27) M28z CAR T cells secreted a 2- to 5-fold greater amount of Th1 cytokines (Fig. S1C) and afforded greater T cell accumulation upon repeated exposure to MSLN+ cells in the absence or presence of exogenous IL-2 (Fig. S1D-E). Based on these findings, we proceeded to evaluate the therapeutic potential of M28z in mice bearing established pleural tumors.

Regional delivery of M28z T cells is more potent than the systemic route

In an orthotopic model of MPM previously established by our laboratory (14, 23, 24, 28), serial bioluminescence imaging (BLI) using firefly-luciferase (fLuc)-transduced MSTO-211H was used to confirm establishment of tumor, equalize tumor burden across intervention groups before initiation of T cell therapy, and measure response to therapy. Mice with established pleural tumor were treated 12 days after tumor inoculation with either a single intravenous or intra-pleural administration of 1×10^5 M28z CAR T cells (Effector to target [E:T] ratio of 1:3000, estimated from tumor burden quantification as previously described)(23, 24). P28z CAR or untransduced T cells were administered at the same dose to demonstrate antigen-specificity and control for alloreactivity and xenoreactivity. Treatment with intravenous M28z T cells at this dose resulted in marginal anti-tumor efficacy (Fig. 1C), hardly exceeding P28z control T cells (Fig. 1D, broken blue line vs. solid black line, MS. 27 vs. 25 days, respectively). In contrast, intra-pleurally administered M28z T cells induced major responses. Tumor burdens were significantly lower by day 7, becoming undetectable by day 11 (Fig. 1C). Median survival was not reached by day 100 (Fig. 1D). Treatment with a higher dose of intravenous M28z T cells (3×10^6, a 30-fold increase, E:T 1:100) reduced tumor burden but did not avert eventual tumor progression (Fig. 1E, S1A), yielding a modest 44-day survival advantage (Fig. 1F, broken blue line). In contrast, a 10-fold lower dose of M28z CAR T cells (3×10^5, E:T 1:1000) administered intra-pleurally rapidly decreased tumor burden within 10 days of administration (Fig. 1E, S1A)

and did not reach median survival by day 200 (solid blue line, Fig. 1F). Experimental results were similar with T cells from 3 different donors, arguing against a significant impact of alloreactivity, if any.

Unlike systemic delivery, intra-pleural T cell administration promotes prompt M28z T cell expansion and differentiation

The long-term tumor-free survival observed with regional CAR T-cell therapy, even at a dose 30-fold lower than that used intravenously, prompted us to investigate T cell tumor infiltration, expansion, and persistence following intra-pleural vs intravenous administration. To this end, we first performed tumor and T cell noninvasive, quantitative BLI. All mice were treated with a single dose of T cells (1×10^6) co-expressing M28z and enhanced firefly luciferase (effLuc). Within 24h of administration, intra-pleural delivery resulted in a rapid increase in pleural M28z T cell accumulation, 10-fold greater than via intravenous delivery (Fig. 2A). This rapid and sustained accumulation occurred with M28z (Fig. 2B, blue line) but not P28z T cells. Intravenously administered M28z T cells yielded signal comparable to intra-pleurally delivered T cells after 5 to 7 days. Rising T cell BLI signal paralleled tumor burden regression recorded by concomitant tumor BLI decrease. Serial immuno-histochemical analyses confirmed the T cell accumulation kinetics (Fig. S2B). Further flow cytometric analysis of the T cell to tumor cell ratio revealed a similar accumulation of CAR T cells at initial time points (day 3-5) when comparing the two routes of administration, which however diverged thereafter, steadily increasing in the case of intra-pleurally delivered T cells but diminishing in the systemically treated mice (Fig. 2C). Consistent with differential acquisition of effector functions, we observed marked differences in the pleural CD4/CD8 ratio and the pattern of CD62L expression (L-selectin), a marker down-regulated upon T-cell activation and effector memory formation (29). While intra-pleural administration maintained a balanced CD4/CD8 ratio, intravenous administration resulted in significantly lesser CD8+ accumulation (Fig. 2C and 2D). The equal distribution of CD4+ and CD8+ T cells seen within the spleen of these mice indicates that the reduced intra-tumoral CD8+ accumulation is not due to a systemic absence of CD8+ T cells. Furthermore, most intravenously administered CD4+ T cells demonstrated a non-activated (CD62L+) T-cell phenotype 1 week after administration. In contrast, a large proportion of intra-pleurally administered CD4+ T cells exhibited an activated CD62L- phenotype (Fig. 2F). CD8+ M28z T cells showed a similar reduction in CD62L expression in either case (Fig. 2F), establishing that differential activation primarily affected the activation of CD4+ T cells and the concomitant accumulation of CD8+ T cells.

Regionally primed M28z T cells support potent, systemic, tumor specific responses

To assess whether intrapleurally administered T cells provide systemic tumor protection, we treated mice bearing MSLN+ pleural tumor expressing firefly luciferase as well as MSLN+ and MSLN− flank tumors (right MSLN+ and left MSLN−, Fig. 3A, left) with intra-pleural M28z T cells expressing Gaussia luciferase. Fifteen days after T cell administration, BLI with coelenterazine demonstrated residual T cells in the pleural cavity and T-cell accumulation in the MSLN+ right-flank tumor (Fig. 3A, center) but not the MSLN− left-flank tumor. Tumor imaging with D-Luciferin on the following day showed eradication of pleural tumor, regression of the MSLN+ right-flank tumor and progression of the MSLN−

left-flank tumor (Fig. 3A, right). Furthermore, we investigated whether intra-pleurally administered CAR T cells could traffic to the peritoneal cavity, a potential site of mesothelioma dissemination. In this dual pleural/peritoneal disease model, intra-pleurally administered M28z T cells rapidly accumulated (days 1–2) and at a higher number than intravenously administered T cells (Fig. 3B and C).

Intrapleurally administered M28z T cells remain functional for at least 100 days

Having demonstrated rapid activation of regionally dispensed M28z T cells and their efficient extra-thoracic redistribution, we further examined their persistence and function. After establishing large pleural tumor burdens over 18 days, we administered Mz, M28z or P28z T cells into the pleural cavity at a low dose of 3×10^5 CAR+ T cells (E:T, 1:1000). Treatment with M28z T cells induced a uniform reduction in tumor bioluminescence to background emission levels, as well as long-term tumor-free survival (median survival not reached vs. 63 days in Mz vs. 36 days in P28z, P=0.01, Fig 4). Serial assessment of CAR+ T cell counts in the peripheral blood of treated mice demonstrated increased T-cell persistence in M28z-treated mice when compared to Mz treated mice (50 days after T-cell infusion; Fig. 4B). Similar results of T-cell persistence were obtained using 3 separate T-cell doses (3×10^6, 1×10^6, and 3×10^5 administered CAR+ T cells). Phenotype assessment of persisting T cells demonstrated progressive and predominant enrichment in CD4+ T cells 30 days after T-cell infusion in both Mz- and M28z-treated mice (Fig. 4C). This gradual CD4+ enrichment was observed at all 3 T cell doses in both spleen and blood.

We next assessed the functional status of persisting T cells by performing a tumor re-challenge experiment. Mice with established MSLN+ pleural tumors were intra-pleurally administered either 3×10^5 Mz or M28z T cells to eradicate pleural tumor and promote long term survival. Eighty-seven days after initial T-cell injection, either MSLN+ or MSLN- tumor cells (1×10^6) were administered into the peritoneal cavity to long-term survivors and tumor burden was monitored using BLI. At the time of rechallenge, persisting T cells were predominantly effector memory (CD45RA-CD62L-) cells (Fig. 5A) as evidenced by FACS analysis in representative mice. After an initial increase in tumor burden in all mice, antigen-specific control of tumor burden was seen in both the Mz and M28z T-cell–treated mice, most markedly in M28z-treated mice (Fig 5B). We then sought to examine the T cell proliferative response on tumor challenge. Mice from all groups were sacrificed 16 days after rechallenge, and spleens were harvested for FACS analysis. Mice initially treated with M28z T cells and rechallenged with MSLN+ tumor showed a 4-fold higher T cell expansion than those rechallenged with MSLN- tumor (Fig. 5C). The greater T cell accumulation was predominantly attributable to the CD4+ subpopulation in the M28z group (Fig. 5D).

Early antigen activation of CD4+ M28z T cells is essential for enhancing CAR T cell efficacy

To assess the relative contribution of CD28 costimulation to CD4+ and CD8+ cytokine and proliferative responses, we stimulated CD4+, CD8+, and bulk T cells transduced with either Mz or M28z with MSLN+ tumor cells and quantified the secretion of Th1 cytokines and proliferation. Compared with CD8+ T cells, CD4+ T cells transduced with Mz had increased levels of Th1 cytokine secretion (Fig. 6A). CD28-costimulated CD4+ T cells secreted 11- to

50-fold higher levels of cytokines than CD8+ T cells, showing that cytokine secretion is strongly enhanced in CD28-costimulated T cells, particularly in CD4+ T cells. As expected, repeated stimulation with MSLN+ targets did not induce T-cell expansion in either the CD4+ or CD8+ Mz T-cell population and rather rapidly induced a decline in T cell number upon antigen stimulation in the absence of exogenous IL-2 (Fig. 6B). In contrast, CD4+ M28z T cells expanded >20-fold greater mean proliferation by the third stimulation, compared with a 2-fold increase in CD8+ M28z T cells ($P<0.001$). The importance of CD4+ CAR T cells in supporting M28z CAR T-cell function was further demonstrated by the robust accumulation of CD8+ M28z T cells when cocultured with CD4+ M28z T cells and stimulated by MSLN+ targets (3-fold greater accumulation; $P<0.001$; Fig. 6C). To further confirm the potentiating function of CD4+ M28z CAR T cells *in vivo*, CD8+ M28z CAR T cells were transduced with effLuc (to monitor T-cell accumulation in pleural tumor–bearing mice). CD8+ M28z CAR T cells had significantly enhanced *in vivo* accumulation when administered with CD4+ M28z T cells, as determined by tracking of T-cell signal emission by BLI (2.3- vs. 1.2-fold increase in T-cell bioluminescent signal at 72 h; Figs. 6D-E).

The enhanced anti-tumor efficacy of pleurally administered M28z T cells could be explained by an earlier antigen-activation of CD4+ M28z T cells which may lead to optimal cytokine secretion to sustain the expansion of both the CD4+ and CD8+ CAR T-cell subsets. In order to demonstrate the influence of early antigen-activation, we performed *in vitro* accumulation experiments described above utilizing pre-activated CD4+M28z T cells (pre-activated once on MSLN+ tumor cells 24hrs prior). CD4+ CAR T-cell pre-activation resulted in an enhancement in both CD4+ and CD8+ accumulation *in vitro* compared to the experimental condition where CD4+ T cells are antigen exposed simultaneously with CD8+ T cells (Fig. 6F).

CD4+ CAR T cells demonstrate CD28-dependent granzyme/perforin-mediated cytotoxicity

We next investigated the cytotoxic potential of M28z CAR T cells. Purified CD8+ T cells demonstrated rapid cytotoxicity over 4 hrs (Fig. 7A, left). CD4+ M28z+ T cells had lower rapid cytotoxic potential but reached equivalent levels to CD8+ M28z+ T cells by 18 hrs. CD28 costimulatory signaling enhanced lysis by CD4+ M28z CAR T cells by 13-16% at multiple E:T ratios ($P<0.001$; Fig. 7B) but did not consistently enhance CD8+ T cell-mediated cytolysis ($P=0.07$). Transfer of cytokine-rich supernatant obtained from stimulated CD4+ M28z T cells added at the time of ^{51}Cr-release assay enhanced the cytotoxicity of both CD4+ M28z T cells (5%–23% enhancement; $P<0.0001$; Fig. 7C) and CD8+ M28z CAR T cells (5%–30% enhancement; $P<0.001$). Transfer of supernatant alone or addition of supernatant to P28z control T cells did not result in lysis (Fig. 7C). We therefore conclude that the M28z CAR favors formation of cytotoxic CD4+ T cell effectors and helps CD8+ T cell cytoxicity in CD4-dependent manner.

With direct lysis of tumor targets by cytokine-rich supernatant excluded, we next sought to determine which of two cell contact–dependent lytic mechanisms (Fas receptor/Fas ligand or granzyme/perforin pathway) were responsible for CAR T-cell cytotoxicity. Antibody blockade of Fas ligand/Fas receptor (FasL/FasR) interaction did not reduce target cell lysis by either Mz or M28z CAR T cells ($P>0.05$; Fig. S3A, left and middle). Flow cytometric

analysis confirmed FasL expression by CAR T cells and FasR expression on MSLN+ tumor (Fig. S3B). MSLN+ cells are indeed susceptible to FasL-mediated cytotoxicity, and the αFasL antibody used in these experiments blocked this effect (Fig. S4A, right). Blockade of granzyme release by the addition of the calcium chelator EGTA to T-cell/tumor-cell coculture reduced CAR-mediated lysis in all groups tested (Fig. 7D), demonstrating that CAR T-cell cytotoxicity is dependent on the perforin/granzyme pathway. The most prominent reduction in lysis was seen in the Mz (mean reduction, 27.6% vs. 17.6% for M28z) and CD8+ (29.4% for CD8+ Mz vs. 15.3% for CD4+ Mz; 24.2% for CD8+ M28z vs. 11.1% for CD4+ M28z) T cell groups. Expression of granzymes A and B in resting peripheral blood mononuclear cells (PBMCs) was primarily restricted to CD8+ T cells, in concordance with the results of previous studies (Figs. 7E and S4C). Granzyme A expression is not significantly altered following PHA stimulation and MSLN-specific stimulation of CAR transduced T cells (Fig. S4D). Granzyme B was expressed in >95% of CD4+ and CD8+ M28z CAR T cells within 18 h after stimulation with MSLN-expressing tumor cells. CD8+ M28z T cells had a 1.8-fold increase in MFI after 4-h coculture, and granzyme B expression was further upregulated to 2.6-fold during the final 12 h. With CD4+ M28z T cells, however, granzyme B expression was upregulated to a much greater degree during the final 12 h of culture (1.5-fold during the first 4 h, to 3.7-fold during the final 12 h). These findings may explain the delayed lysis kinetics displayed by CD4+ CAR T cells. Furthermore, M28z enhanced granzyme B expression in both CD4+ and CD8+ T-cell subsets (Fig. 7E, expression following 18 h of coculture), possibly explaining the enhanced cytotoxicity seen with CD4+ M28z T cells compared with CD4+ Mz T cells (Fig. 7B).

Regionally administered CD4+ CAR T cells are efficacious alone and mediate functional persistence

Our observations of a potent CD4+ M28z *in vitro* effector function and CD4+ predominant long-term immunity led us to hypothesize that CD4+ M28z T cells would demonstrate *in vivo* efficacy in the absence of CD8+ T cells. Tumor-bearing mice were treated with CD4+ M28z, CD8+ M28z, or bulk unsorted M28z T cells administered into the pleural cavity at 3 different doses following 18 days of tumor growth (Figs. 8A and 8B). In P28z treated mice, the tumor burden steadily progressed until mice had to be sacrificed (median survival, 28 days). Treatment with CD4+ M28z and bulk M28z CAR T cells (3×10^5; E:T, 1:1000) resulted in tumor eradication in 100% of mice, with mice remaining tumor free through 200 days of follow-up. Treatment with CD8+ M28z T cells extended survival by 83 days only (111 vs. 28 days; P=0.003; Fig. 8B) and achieved tumor eradication in only 3 of 7 mice. Even at the lower doses, CD4+ M28z CAR T cells had higher efficacy than CD8+ CAR T cells (1×10^5: E:T, 1:3000, 112 vs. 67 days [P=0.04]; 3×10^4: E:T, 1:10000, 160 vs. 37 days [P=0.001]). These results illustrate that CD4+ CAR T cells alone are superior to CD8+ CAR T cells alone, although they are not as effective as combined CD4+ and CD8+ T cells.

Finally, to address whether CD4+ T cells can establish long-term functional persistence when administered without CD8+ T cells, we performed peritoneal tumor re-challenge in mice 196 days after initial intra-pleural administration of CD4+ sorted or bulk M28z T cells. Although there was an initial increase in tumor burden with persisting CD4+ M28z T cells

compared to the bulk population containing both CD4+ and CD8+, tumors then regressed, and subsequent tumor growth was controlled for >4 weeks (Fig. 8C).

Discussion

We took advantage of an orthotopic MPM model that faithfully mimics human disease (14, 23, 24, 28) to evaluate two routes of administration to treat malignant pleural disease with MSLN-targeted T cells. We found that intra-pleurally administered CAR T cells vastly outperformed systemically infused T cells, inducing long-term complete remissions with less than 30-fold fewer M28z CAR T cells. Regionally administered CAR T cells displayed rapid and robust T-cell expansion, resulting in effective T cell differentiation and systemic tumor immunity. This superior efficacy was dependent on early CD4+ T cell activation and associated with a higher intra-tumoral CD4/CD8 cell ratio and long-term memory. In contrast, intravenously delivered CAR T cells, even when accumulated at equivalent numbers in the pleural tumor, did not achieve comparable activation, tumor eradication or persistence. The translational relevance of these findings is further increased by the use of human T cells and CARs as these will be utilized in clinical studies based on the results reported herein.

In our studies, we intra-pleurally administered MSLN-targeted CAR T cells to mice bearing established pleural tumors (12-18 days post-inoculation, control mice die by day 25-36). Using tumor and T cell noninvasive imaging, we demonstrated that intra-pleurally administered CAR T cells (1) efficiently infiltrate throughout the tumor in the chest, (2) become potent effector cells that eradicate pleural tumor at doses 30-fold lower than those used in intravenous therapy, and (3) migrate out of the pleural cavity, circulate, and accumulate in extra-thoracic tumor sites. While the immediate location of regionally administered cells evidently circumvents the obligate circulation and transient pulmonary sequestration of intravenously administered T cells, the intra-pleurally administered T cells differed from systemically recruited T cells in 1) the level of CD8 T cell accumulation and 2) the rapidity of kinetics of effector differentiation, as reflected by CD62L down-regulation. The initial lack of pleural CD8+ T cell accumulation is not caused by overall CD8+ T cell disappearance, as CD8+ T cells persisted in the spleen of mice over 7 days after intravenous administration. Their poor recruitment could be in part due to suboptimal expression of chemokine receptor or adhesion molecules required for their trafficking. However, even though pleural accumulation may be enhanced by forced expression of transduced CCR-2 in CAR T cells (22), regional therapy with CAR T cells bypasses trafficking restrictions, if any, and enables, without additional T cell engineering, highly efficient redistribution to other tumor locations with greater efficacy than intravenously administered T cells. Furthermore, a single dose of regional CAR T-cell therapy established long-term tumor immunity (up to 200 days after T cell administration), providing effective protection against tumor re-challenge.

This systemic benefit of regional CAR T-cell therapy is reminiscent of the abscopal effect of loco-regional radiation therapy(30, 31) and intra-tumoral oncolytic viral therapy(32) for solid malignancies, in which a local inflammatory response may generate specific immunity and effectively impact distant tumor sites. Intrapleurally administered CAR T cells migrate

out of the pleural cavity and are directly visualized at extrapleural tumor sites as early as 24 to 72 h after administration. Thus early T-cell activation has a beneficial effect on CAR T-cell biodistribution. The rapid acquisition of a $CD62L^-$ phenotype may account for their efficient subsequent trafficking to metastatic sites (29). The extensive lymphovascularity of pleural mesothelioma (23) in our orthotopic model, which contrasts with that of flank tumors, which typically undergo central necrosis upon growth, may contribute to such efficient T cell activation and redistribution.

The remarkable ability of intrapleurally administered T cells to circulate and persist within the periphery opens new avenues of treatment for metastatic cancers with accessible tumor sites, which may serve as "regional charging and distribution centers" for CAR T cell therapy. These include cancers that metastasize to the pleural cavity, such as lung and breast cancers, as well as those that metastasize to the peritoneal cavity, such as pancreatic and ovarian cancers. In addition to intrapleural or intraperitoneal administration, our findings raise the prospect that other regional adoptive T cell therapy approaches such as hepatic artery infusion, regional limb perfusion or intracranial administration (33-35)may provide superior efficacy. More conservatively, these regional and/or intratumoral delivery approaches are highly applicable to other MSLN-expressing sold cancers, which include ovarian, pancreatic, colorectal, lung, triple-negative breast, esophageal, gastric, cholangio and thymic cancer (14-16, 36-41). This approach may at the very least decrease the T cell dose requirement, presenting an advantage when high numbers of CAR T cells are not attainable (due to low-yield apheresis, poor *ex vivo* expansion or low transduction) and may even obviate the need for systematic apheresis.

The early infiltration and activation of the CD4+ T-cell subset is essential to the observed benefits of regional administration. M28z CAR T cells were multifunctional, displaying potent CD4+ T-cell cytotoxicity as well as helper function supporting T cell effector formation, survival and proliferation. The dual functionality of CD4+ T cells is most clearly demonstrated by the ability of CD4+ effectors to independently eliminate pleural mesothelioma xenografts following regional administration. Their key role in helper function is further supported by the enhanced CD8+ T cell subset observed following pleural administration compared to intravenous administration and the importance of early-antigen activated CD4+ T cells for achieving a CD8+ T-cell proliferative burst. The lesser ability of intravenously administered T cells to achieve potent accumulation of both CD4+ and CD8+ subsets, suggests that M28z CAR T cells are negatively impacted by their delayed arrival at the tumor site.

The critical role of CD28 costimulation provided through the CAR is revealed in several ways. M28z T cells eliminated large pleural tumors even at low T-cell doses. The intrapleural T cell doses we used (3×10^5 M28z T cells in most experiments) is a markedly lower dose than used in other mesothelioma xenografts studies (20-22), and is comparable to doses used in current clinical trials for hematologic malignancies (9, 10) and solid tumors (42, 43) (Suppl Table 1). Compared to Mz T cells, M28z T cells provided superior tumor control and robust proliferation upon tumor rechallenge >100 days after intrapleural administration. The potentiating properties of CD28 signaling are particularly notable in the CD4+ subset, as demonstrated by their superior cytokine secretion and proliferation, relative

to CD8+ T cells. Interestingly, the CD28/CD3ζ CAR was essential to induce efficient CD4+ T cell-mediated cytotoxicity by a perforin/granzyme-dependent pathway. It is well established that CD4+ T cells require a higher-avidity interaction to mediate effector functions compared to CD8+ T cells (44, 45). CD28/CD3ζ CAR engineering may thus be particularly suited for generating multifunctional CD4+ T cells that are capable of T cell help and cytotoxicity (46).

The enhanced localization and activation of mesothelin-targeted CAR T cells in the vicinity of normal tissues that express low levels of mesothelin may increase the hypothetical risk of "on-target off-tumor" toxicities such as pleuritis and pericarditis. However, mesothelin expression is markedly higher in tumor tissues compared to normal tissues, as we previously reported.(15, 16, 47) Since CAR T cell activation is stronger in the presence of higher antigen density, CAR T cells are expected to more strongly respond to tumor than to the normal tissue. This is supported by our *in vitro* studies using an isogenic target (Figure S5) and others.(46, 48) It is also noteworthy that histopathological studies in mice treated with mesothelin-targeted CAR T cells did not reveal inflammatory changes in the pleura or pericardium. Furthermore, clinical studies targeting mesothelin with immunotoxins have not shown toxicity to normal tissues in over 100 patients.(19, 49, 50) The reported toxicity observed in a patient treated with mesothelin-targeted CAR T cells (an anaphylactic shock) was due to an antibody response to the CAR, which comprises a murine scFv.(51) Our M28z CAR is comprised of human sequences only.(52) Nonetheless, we believe that additional strategies are necessary to limit or prevent reactivity against normal tissue. While lymphotoxic corticosteroids can sometimes eliminate CAR T cells,(11) we will proceed to the clinic utilizing a suicide gene.(53) Suicide genes such as iCaspase-9,(53) EGFR mutation(54) and herpes simplex virus thymidine kinase-(55) mediate rapid T cell elimination following administration of a prodrug or antibody. We may also pursue, if necessary, alternative strategies designed to prevent reactivity against normal tissues utilizing combinatorial antigen recognition or inhibitory receptors.(56-58) Another strategy to limit CAR T cell toxicity is to transiently express the CAR using mRNA electroporation,(21, 59) albeit at the expense of CAR T cell persistence and requiring multiple T-cell administrations to attain efficacy.

In the reported study, we used immunodeficient mice with human cancer cells and human T cells in order to facilitate direct clinical translation of our findings and the human-based CAR vectors to clinical trials as we previously did for CD19- and PSMA- targeted CAR T-cell therapies.(11, 60, 61) The interactions between adoptively transferred cells and the endogenous immune system investigated in an immunocompetent mouse model will extend the significance of our observations.

Based on the data presented herein, we designed a phase I clinical trial to evaluate the safety of intrapleural administration of MSLN-targeted CAR T cells. Patients with primary pleural malignancy or secondary pleural malignancies from lung and breast cancers overexpressing MSLN, which we have shown to have more aggressive disease (15, 47), will be enrolled on this trial. MSLN-targeted CAR T cells will be delivered through intrapleural catheters, an approach we developed to be the standard of care in managing patients with malignant pleural effusions (62). The regional administration of biological agents such as cytokines

(63) and oncolytic virus (64) has been previously translated to the clinic with success. Our studies strongly support that regional CAR T cell administration to subjects with MPM will result in greater T cell anti-tumor potency with reduced T cell doses, owing in part to early CD4+ T cell activation and the systemic benefits that ensue.

Materials and Methods

Study design

The purpose of this study was to create an optimal T cell immunotherapy for solid malignancies. We designed mesothelin-targeted chimeric antigen receptors that, when transduced into human T cells, provide tumor antigen recognition and antigen-specific effector function. *In vitro*, we analyzed (i) cytotoxicity, (ii) cytokine secretion, and (iii) T cell proliferation. *In vivo* experiments analyzed strategies for optimizing T-cell therapy using live imaging of both T cells and tumor. We used immunodeficient mice with human cancer cells and human T cells in order to validate and facilitate the translation of our M28z CAR to the clinic, as we previously did for CD19 (Brentjens, NM, 2003) and PSMA (Gade, CR, 2005). The study of mechanistic interactions between CAR T cells and the endogenous immune system would be best studied in an immunocompetent mouse model, which would however have to utilize a murine CAR differing from its clinically relevant counterpart. The experimental procedures were approved by the Institutional Animal Care and Use Committee of Memorial Sloan-Kettering Cancer Center (MSKCC). Each experiment was performed multiple times using different donor T cells (T cells were never pooled). We present data using a representative experiment (with sample replicates of more than three) to avoid confounding variables such as differences due to transduction efficiencies, donor-related variability, and E:T ratios.

Cell lines—MSTO-211H (human pleural mesothelioma) and EL4 (murine thymoma) cells were retrovirally transduced to express the GFP/firefly luciferase fusion protein (MSTO GFP-ffLuc+). These cells were then transduced with the human MSLN-variant 1 subcloned into a SFG retroviral vector to generate MSTO MSLN+ GFP-ffLuc+.

Gamma-retroviral vector construction and viral production—To generate MSLN-specific CARs, we engineered a fusion protein encoding a fully human scFv, m912 (kindly provided by D. Dimitrov, NCI-Frederick)(25) linked to the human CD8 leader peptide and the CD8/CD3ζ or CD28/CD3ζ sequences as previously described.(65) Within the SFG gamma-retroviral vector backbone (kindly provided by I Riviere, MSKCC), we inserted an internal ribosomal entry site to facilitate bicistronic expression of CARs with humanized recombinant GFP reporter gene. The Mz, M28z, and P28z-encoding plasmids were then transfected into 293T H29 packaging cell lines as previously described (66).

T-cell isolation, gene transfer, and CD4/CD8 isolation—Peripheral blood leukocytes were isolated from the blood of healthy volunteer donors under an institutional review board–approved protocol. PHA-activated PBMCs were isolated by low-density centrifugation on Lymphoprep. Two days after isolation, PBMCs were transduced with 293T RD114–produced supernatant containing Mz, M28z, or P28z vectors for 1 h on plates

coated with 15 μg/mL retronectin daily for 2 days. After allowing 3 days for vector expression, transduced PBMCs were maintained in 20 units/mL IL-2. Transduction efficiencies were determined by flow cytometric analysis. Pure populations of CD4+ and CD8+ T cells were obtained through negative selection protocols using Dynabeads Untouched Human CD4 and CD8 T-cell isolation kits.

Cytotoxicity assays—The cytotoxicity of T cells transduced with a CAR or vector control was determined by standard ^{51}Cr-release assays as previously described (67).

Orthotopic pleural mesothelioma animal model and in vivo assessments—To develop the orthotopic mouse model of pleural mesothelioma, female NOD/SCID gamma mice at 6 to 10 weeks of age were used. All procedures were performed under approved Institutional Animal Care and Use Committee protocols. Mice were anesthetized using inhaled isoflurane and oxygen and were administered bupivacaine for analgesia. Direct intrapleural injection of 1×10^5 to 1×10^6 tumor cells in 200 μL of serum-free media via a right thoracic incision was performed to establish orthotopic MPM tumors, as previously described (24, 68-70). In total, 3×10^4 to 3×10^6 transduced T cells were adoptively transferred into tumor-bearing mice, with 200 μL of serum-free media, into the thoracic cavity of mice by direct intrapleural injection or systemically by tail vein injection. Peripheral blood was obtained by retro-orbital bleeding.

Cytokine detection assays—Cytokine-release assays were performed by coculturing 5×10^5 to 5×10^3 T cells transduced with M28z, Mz, or control vector with 5×10^3 target cells in 200 uL of media in 96-well round-bottom plates as triplicates. After 6 to 24 h of coculture, supernatants were collected. Cytokine levels were determined using multiplex bead Human Cytokine Detection kit.

T-cell proliferation assays—In total, 1×10^6 to 3×10^6 T cells transduced with M28z, Mz, or P28z were stimulated over irradiated MSTO-211H cells with or without MSLN expression and were plated in 6- or 24-well tissue culture plates at a density of 1×10^5 to 3×10^5 cells/well. Proliferation assays were performed in the absence or presence of 20 U/mL exogenous IL-2, as noted. Cells were counted every 4 or 7 days and then overlaid on irradiated MSTO-211H cells with or without MSLN expression. Cell number versus time was plotted for each T-cell group, and phenotypes were determined by flow cytometric analysis.

Histologic analysis and immunostaining—Histopathologic evaluation of tumors was performed after hematoxylin and eosin staining of paraffin-embedded, 4% paraformaldehyde–fixed tissue samples. Immunohistochemical analysis for human MSLN was performed with a mouse anti-human MSLN IgG. Human anti-CD3 staining was performed with a mouse anti-human CD3 IgG.

Flow Cytometry—Human MSLN expression was detected using a PE-conjugated or APC-conjugated anti-human MSLN rat IgG_{2a}. T-cell phenotypes were determined with monoclonal antibodies for CD3, CD4, CD8, CD62L, CD25, CD27 and CD45RA. Subsequent flow cytometry for GFP, MSLN expression, and T-cell phenotype analysis was

performed on an LSRII cytometers and analyzed using FlowJo analysis software. Mouse tissues were processed as follows: tissues were weighed and harvested into ice-cold RPMI-1640. The tissues were manually morselized with a scalpel and then mechanically disaggregated through 40-100 um filters. Samples were resuspended and 2 $\times 10^6$events were recorded on FACS.

Quantitative and T-cell BLI In vivo—BLI in mice was performed using a single intraperitoneal dose of 150mg/kg D-Luciferin for firefly or effLuc reporter gene (Kindly provided by Dr Patrick Hwu, Texas)(23, 71). Cells transduced with M28z and a Gaussia luciferase reporter gene were imaged with a single intravenous dose of 15ug native coelentereazine resuspended in 150 ul of propylene glycol:PBS (1:1)(72). BLI data were analyzed using Living Image 2.60 software and BLI signal reported as total flux (photons/s). BLI flux (photon/s) was then determined as the average of ventral and dorsal images with Microsoft Excel (Microsoft Corp., WA) and analyzed with GraphPad Prism (GraphPad Software, Inc., CA).

Statistical methods—Data are presented as means +/- SD or SEM as stated in the figure legends. Results were analyzed by unpaired Student't t test (two-tailed) with Bonferroni correction for multiple comparisons where applicable. Survival curves were analyzed with log-rank test. Statistical significance was defined as $P < 0.05$. All exact P values are provided in the Supplemental Materials. All statistical analysis were performed with Prism software version 6.0 (GraphPad).

Supplementary Material

Refer to Web version on PubMed Central for supplementary material.

Acknowledgments

We are grateful to Drs Dimiter Dimitrov and Yang Feng from NCI for providing us the mesothelin scFv under MTA. The effLuc reporter gene was kindly provided by Dr Patrick Hwu, from MD Anderson Cancer Center in Houston, Texas. We are thankful to Dr. Camelia Sima for all of the biostatistical analysis presented in this manuscript. We also thank Alex Torres of the MSK Thoracic Surgery Service for his editorial assistance.

Funding: This work was supported, in part, by the American Association for Thoracic Surgery Third Edward D. Churchill Research Scholarship; William H. Goodwin and Alice Goodwin, the Commonwealth Foundation for Cancer Research and the Experimental Therapeutics Center; the National Cancer Institute (grants R21 CA164568-01A1, R21 CA164585-01A1, and 2T32CA9501-26A1); the U.S. Department of Defense (grants PR101053 and LC110202); and the NIH/NCI Cancer Center Support Grant P30 CA008748; and Stand Up To Cancer—Cancer Research Institute Cancer Immunology Translational Cancer Research Grant (SU2C-AACR-DT1012). Stand Up To Cancer is a program of the Entertainment Industry Foundation administered by the American Association for Cancer Research.

References

1. Antony VB, Loddenkemper R, Astoul P, Boutin C, Goldstraw P, Hott J, Rodriguez Panadero F, Sahn SA. Management of malignant pleural effusions. Eur Respir J. 2001; 18:402–419. [PubMed: 11529302]
2. Robinson BW, Musk AW, Lake RA. Malignant mesothelioma. Lancet. 2005; 366:397–408. [PubMed: 16054941]

3. Anraku M, Cunningham KS, Yun Z, Tsao MS, Zhang L, Keshavjee S, Johnston MR, de PM. Impact of tumor-infiltrating T cells on survival in patients with malignant pleural mesothelioma. J Thorac Cardiovasc Surg. 2008; 135:823–829. [PubMed: 18374762]
4. Yamada N, Oizumi S, Kikuchi E, Shinagawa N, Konishi-Sakakibara J, Ishimine A, Aoe K, Gemba K, Kishimoto T, Torigoe T, Nishimura M. CD8+ tumor-infiltrating lymphocytes predict favorable prognosis in malignant pleural mesothelioma after resection. Cancer Immunol Immunother. 2010; 59:1543–1549. [PubMed: 20567822]
5. Suzuki K, Kadota K, Sima CS, Sadelain M, Rusch VW, Travis WD, Adusumilli PS. Chronic inflammation in tumor stroma is an independent predictor of prolonged survival in epithelioid malignant pleural mesothelioma patients. Cancer Immunol Immunother. 2011; 60:1721–1728. [PubMed: 21769693]
6. Bograd AJ, Suzuki K, Vertes E, Colovos C, Morales EA, Sadelain M, Adusumilli PS. Immune responses and immunotherapeutic interventions in malignant pleural mesothelioma. Cancer Immunol Immunother. 2011; 60:1509–1527. [PubMed: 21913025]
7. Adusumilli PS. Translational immunotherapeutics: Chemoimmunotherapy for malignant pleural mesothelioma. Cancer. 2014
8. Kochenderfer JN, Dudley ME, Carpenter RO, Kassim SH, Rose JJ, Telford WG, Hakim FT, Halverson DC, Fowler DH, Hardy NM, Mato AR, Hickstein DD, Gea-Banacloche JC, Pavletic SZ, Sportes C, Maric I, Feldman SA, Hansen BG, Wilder JS, Blacklock-Schuver B, Jena B, Bishop MR, Gress RE, Rosenberg SA. Donor-derived CD19-targeted T cells cause regression of malignancy persisting after allogeneic hematopoietic stem cell transplantation. Blood. 2013; 122:4129–4139. [PubMed: 24055823]
9. Brentjens RJ, Davila ML, Riviere I, Park J, Wang X, Cowell LG, Bartido S, Stefanski J, Taylor C, Olszewska M, Borquez-Ojeda O, Qu J, Wasielewska T, He Q, Bernal Y, Rijo IV, Hedvat C, Kobos R, Curran K, Steinherz P, Jurcic J, Rosenblat T, Maslak P, Frattini M, Sadelain M. CD19-targeted T cells rapidly induce molecular remissions in adults with chemotherapy-refractory acute lymphoblastic leukemia. Science translational medicine. 2013; 5:177ra138.
10. Grupp SA, Kalos M, Barrett D, Aplenc R, Porter DL, Rheingold SR, Teachey DT, Chew A, Hauck B, Wright JF, Milone MC, Levine BL, June CH. Chimeric antigen receptor-modified T cells for acute lymphoid leukemia. N Engl J Med. 2013; 368:1509–1518. [PubMed: 23527958]
11. Davila ML, Riviere I, Wang X, Bartido S, Park J, Curran K, Chung SS, Stefanski J, Borquez-Ojeda O, Olszewska M, Qu J, Wasielewska T, He Q, Fink M, Shinglot H, Youssif M, Satter M, Wang Y, Hosey J, Quintanilla H, Halton E, Bernal Y, Bouhassira DC, Arcila ME, Gonen M, Roboz GJ, Maslak P, Douer D, Frattini MG, Giralt S, Sadelain M, Brentjens R. Efficacy and toxicity management of 19-28z CAR T cell therapy in B cell acute lymphoblastic leukemia. Science translational medicine. 2014; 6:224ra225.
12. Sadelain M, Brentjens R, Riviere I. The basic principles of chimeric antigen receptor design. Cancer discovery. 2013; 3:388–398. [PubMed: 23550147]
13. Jensen MC, Riddell SR. Design and implementation of adoptive therapy with chimeric antigen receptor-modified T cells. Immunol Rev. 2014; 257:127–144. [PubMed: 24329794]
14. Servais EL, Colovos C, Rodriguez L, Bograd AJ, Nitadori J, Sima C, Rusch VW, Sadelain M, Adusumilli PS. Mesothelin overexpression promotes mesothelioma cell invasion and MMP-9 secretion in an orthotopic mouse model and in epithelioid pleural mesothelioma patients. Clin Cancer Res. 2012; 18:2478–2489. [PubMed: 22371455]
15. Kachala SS, Bograd AJ, Villena-Vargas J, Suzuki K, Servais EL, Kadota K, Chou J, Sima CS, Vertes E, Rusch VW, Travis WD, Sadelain M, Adusumilli PS. Mesothelin overexpression is a marker of tumor aggressiveness and is associated with reduced recurrence-free and overall survival in early-stage lung adenocarcinoma. Clin Cancer Res. 2014; 20:1020–1028. [PubMed: 24334761]
16. Rizk NP, Servais EL, Tang LH, Sima CS, Gerdes H, Fleisher M, Rusch VW, Adusumilli PS. Tissue and serum mesothelin are potential markers of neoplastic progression in Barrett's associated esophageal adenocarcinoma. Cancer Epidemiol Biomarkers Prev. 2012; 21:482–486. [PubMed: 22237988]
17. Villena-Vargas J, Adusumilli PS. Mesothelin-targeted immunotherapies for malignant pleural mesothelioma. Annals of cardiothoracic surgery. 2012; 1:466–471. [PubMed: 23977538]

18. Pastan I, Hassan R. Discovery of Mesothelin and Exploiting It as a Target for Immunotherapy. Cancer Res. 2014

19. Hassan R, Miller AC, Sharon E, Thomas A, Reynolds JC, Ling A, Kreitman RJ, Miettinen MM, Steinberg SM, Fowler DH, Pastan I. Major cancer regressions in mesothelioma after treatment with an anti-mesothelin immunotoxin and immune suppression. Science translational medicine. 2013; 5:208ra147.

20. Carpenito C, Milone MC, Hassan R, Simonet JC, Lakhal M, Suhoski MM, Varela-Rohena A, Haines KM, Heitjan DF, Albelda SM, Carroll RG, Riley JL, Pastan I, June CH. Control of large, established tumor xenografts with genetically retargeted human T cells containing CD28 and CD137 domains. Proc Natl Acad Sci U S A. 2009; 106:3360–3365. [PubMed: 19211796]

21. Zhao Y, Moon E, Carpenito C, Paulos CM, Liu X, Brennan AL, Chew A, Carroll RG, Scholler J, Levine BL, Albelda SM, June CH. Multiple injections of electroporated autologous T cells expressing a chimeric antigen receptor mediate regression of human disseminated tumor. Cancer Res. 2010; 70:9053–9061. [PubMed: 20926399]

22. Moon EK, Carpenito C, Sun J, Wang LC, Kapoor V, Predina J, Powell DJ Jr, Riley JL, June CH, Albelda SM. Expression of a functional CCR2 receptor enhances tumor localization and tumor eradication by retargeted human T cells expressing a mesothelin-specific chimeric antibody receptor. Clin Cancer Res. 2011; 17:4719–4730. [PubMed: 21610146]

23. Servais EL, Colovos C, Kachala SS, Adusumilli PS. Pre-clinical mouse models of primary and metastatic pleural cancers of the lung and breast and the use of bioluminescent imaging to monitor pleural tumor burden. Current protocols in pharmacology/editorial board, S J Enna. 2011; Chapter 14(Unit 14):21.

24. Servais EL, Suzuki K, Colovos C, Rodriguez L, Sima C, Fleisher M, Rusch VW, Sadelain M, Adusumilli PS. An in vivo platform for tumor biomarker assessment. PLoS One. 2011; 6:e26722. [PubMed: 22046338]

25. Feng Y, Xiao X, Zhu Z, Streaker E, Ho M, Pastan I, Dimitrov DS. A novel human monoclonal antibody that binds with high affinity to mesothelin-expressing cells and kills them by antibody-dependent cell-mediated cytotoxicity. Molecular cancer therapeutics. 2009; 8:1113–1118. [PubMed: 19417159]

26. Maher J, Brentjens RJ, Gunset G, Riviere I, Sadelain M. Human T-lymphocyte cytotoxicity and proliferation directed by a single chimeric TCRzeta /CD28 receptor. Nature biotechnology. 2002; 20:70–75.

27. Brentjens RJ, Santos E, Nikhamin Y, Yeh R, Matsushita M, La Perle K, Quintas-Cardama A, Larson SM, Sadelain M. Genetically targeted T cells eradicate systemic acute lymphoblastic leukemia xenografts. Clin Cancer Res. 2007; 13:5426–5435. [PubMed: 17855649]

28. Adusumilli PS, Stiles BM, Chan MK, Mullerad M, Eisenberg DP, Ben-Porat L, Huq R, Rusch VW, Fong Y. Imaging and therapy of malignant pleural mesothelioma using replication-competent herpes simplex viruses. The journal of gene medicine. 2006; 8:603–615. [PubMed: 16475242]

29. Sallusto F, Lenig D, Forster R, Lipp M, Lanzavecchia A. Two subsets of memory T lymphocytes with distinct homing potentials and effector functions. Nature. 1999; 401:708–712. [PubMed: 10537110]

30. Reits EA, Hodge JW, Herberts CA, Groothuis TA, Chakraborty M, Wansley EK, Camphausen K, Luiten RM, de Ru AH, Neijssen J, Griekspoor A, Mesman E, Verreck FA, Spits H, Schlom J, van Veelen P, Neefjes JJ. Radiation modulates the peptide repertoire, enhances MHC class I expression, and induces successful antitumor immunotherapy. J Exp Med. 2006; 203:1259–1271. [PubMed: 16636135]

31. Formenti SC, Demaria S. Systemic effects of local radiotherapy. Lancet Oncol. 2009; 10:718–726. [PubMed: 19573801]

32. Zamarin D, Holmgaard RB, Subudhi SK, Park JS, Mansour M, Palese P, Merghoub T, Wolchok JD, Allison JP. Localized oncolytic virotherapy overcomes systemic tumor resistance to immune checkpoint blockade immunotherapy. Science translational medicine. 2014; 6:226ra232.

33. Kitahara T, Watanabe O, Yamaura A, Makino H, Watanabe T, Suzuki G, Okumura K. Establishment of interleukin 2 dependent cytotoxic T lymphocyte cell line specific for autologous brain tumor and its intracranial administration for therapy of the tumor. Journal of neuro-oncology. 1987; 4:329–336. [PubMed: 3494820]

34. Sigurdson ER, Ridge JA, Kemeny N, Daly JM. Tumor and liver drug uptake following hepatic artery and portal vein infusion. J Clin Oncol. 1987; 5:1836–1840. [PubMed: 3681370]
35. Thom AK, Alexander HR, Andrich MP, Barker WC, Rosenberg SA, Fraker DL. Cytokine levels and systemic toxicity in patients undergoing isolated limb perfusion with high-dose tumor necrosis factor, interferon gamma, and melphalan. J Clin Oncol. 1995; 13:264–273. [PubMed: 7799030]
36. Tchou J, Wang LC, Selven B, Zhang H, Conejo-Garcia J, Borghaei H, Kalos M, Vondeheide RH, Albelda SM, June CH, Zhang PJ. Mesothelin, a novel immunotherapy target for triple negative breast cancer. Breast Cancer Res Treat. 2012; 133:799–804. [PubMed: 22418702]
37. Kawamata F, Kamachi H, Einama T, Homma S, Tahara M, Miyazaki M, Tanaka S, Kamiyama T, Nishihara H, Taketomi A, Todo S. Intracellular localization of mesothelin predicts patient prognosis of extrahepatic bile duct cancer. Int J Oncol. 2012; 41:2109–2118. [PubMed: 23064529]
38. Einama T, Homma S, Kamachi H, Kawamata F, Takahashi K, Takahashi N, Taniguchi M, Kamiyama T, Furukawa H, Matsuno Y, Tanaka S, Nishihara H, Taketomi A, Todo S. Luminal membrane expression of mesothelin is a prominent poor prognostic factor for gastric cancer. Br J Cancer. 2012; 107:137–142. [PubMed: 22644300]
39. Hassan R, Laszik ZG, Lerner M, Raffeld M, Postier R, Brackett D. Mesothelin is overexpressed in pancreaticobiliary adenocarcinomas but not in normal pancreas and chronic pancreatitis. Am J Clin Pathol. 2005; 124:838–845. [PubMed: 16416732]
40. Frierson HF Jr, Moskaluk CA, Powell SM, Zhang H, Cerilli LA, Stoler MH, Cathro H, Hampton GM. Large-scale molecular and tissue microarray analysis of mesothelin expression in common human carcinomas. Hum Pathol. 2003; 34:605–609. [PubMed: 12827615]
41. Argani P, Iacobuzio-Donahue C, Ryu B, Rosty C, Goggins M, Wilentz RE, Murugesan SR, Leach SD, Jaffee E, Yeo CJ, Cameron JL, Kern SE, Hruban RH. Mesothelin is overexpressed in the vast majority of ductal adenocarcinomas of the pancreas: identification of a new pancreatic cancer marker by serial analysis of gene expression (SAGE). Clin Cancer Res. 2001; 7:3862–3868. [PubMed: 11751476]
42. Louis CU, Savoldo B, Dotti G, Pule M, Yvon E, Myers GD, Rossig C, Russell HV, Diouf O, Liu E, Liu H, Wu MF, Gee AP, Mei Z, Rooney CM, Heslop HE, Brenner MK. Antitumor activity and long-term fate of chimeric antigen receptor-positive T cells in patients with neuroblastoma. Blood. 2011; 118:6050–6056. [PubMed: 21984804]
43. Beatty GL, Haas AR, Maus MV, Torigian DA, Soulen MC, Plesa G, Chew A, Zhao Y, Levine BL, Albelda SM, Kalos M, June CH. Mesothelin-specific chimeric antigen receptor mRNA-engineered T cells induce anti-tumor activity in solid malignancies. Cancer Immunol Res. 2014; 2:112–120. [PubMed: 24579088]
44. Engels B, Chervin AS, Sant AJ, Kranz DM, Schreiber H. Long-term persistence of CD4(+) but rapid disappearance of CD8(+) T cells expressing an MHC class I-restricted TCR of nanomolar affinity. Mol Ther. 2012; 20:652–660. [PubMed: 22233579]
45. Zhao Y, Bennett AD, Zheng Z, Wang QJ, Robbins PF, Yu LY, Li Y, Molloy PE, Dunn SM, Jakobsen BK, Rosenberg SA, Morgan RA. High-affinity TCRs generated by phage display provide CD4+ T cells with the ability to recognize and kill tumor cell lines. J Immunol. 2007; 179:5845–5854. [PubMed: 17947658]
46. Stone JD, Aggen DH, Schietinger A, Schreiber H, Kranz DM. A sensitivity scale for targeting T cells with chimeric antigen receptors (CARs) and bispecific T-cell Engagers (BiTEs). Oncoimmunology. 2012; 1:863–873. [PubMed: 23162754]
47. Servais EL, Colovos C, Rodriguez LA, Bograd AJ, Nitadori JI, Sima CS, Rusch VW, Sadelain M, Adusumilli PS. Mesothelin overexpression promotes mesothelioma cell invasion and MMP-9 secretion in an orthotopic mouse model and in epithelioid pleural mesothelioma patients. Clin Cancer Res. 2012
48. Lanitis E, Poussin M, Hagemann IS, Coukos G, Sandaltzopoulos R, Scholler N, Powell DJ Jr. Redirected antitumor activity of primary human lymphocytes transduced with a fully human anti-mesothelin chimeric receptor. Mol Ther. 2012; 20:633–643. [PubMed: 22127019]
49. Hassan R, Cohen SJ, Phillips M, Pastan I, Sharon E, Kelly RJ, Schweizer C, Weil S, Laheru D. Phase I clinical trial of the chimeric anti-mesothelin monoclonal antibody MORAb-009 in patients with mesothelin-expressing cancers. Clin Cancer Res. 2010; 16:6132–6138. [PubMed: 21037025]

50. Hassan R, Kindler HL, Jahan T, Bazhenova L, Reck M, Thomas A, Pastan I, Parno J, O'Shannessy DJ, Fatato P, Maltzman JD, Wallin BA. Phase II clinical trial of amatuximab, a chimeric anti-mesothelin antibody with pemetrexed and cisplatin in advanced unresectable pleural mesothelioma. Clin Cancer Res. 2014
51. Maus MV, Haas AR, Beatty GL, Albelda SM, Levine BL, Liu X, Zhao Y, Kalos M, June CH. T cells expressing chimeric antigen receptors can cause anaphylaxis in humans. Cancer Immunol Res. 2013; 1:26–31.
52. Feng Y, Xiao X, Zhu Z, Streaker E, Ho M, Pastan I, Dimitrov DS. A novel human monoclonal antibody that binds with high affinity to mesothelin-expressing cells and kills them by antibody-dependent cell-mediated cytotoxicity. Mol Cancer Ther. 2009
53. Di Stasi A, Tey SK, Dotti G, Fujita Y, Kennedy-Nasser A, Martinez C, Straathof K, Liu E, Durett AG, Grilley B, Liu H, Cruz CR, Savoldo B, Gee AP, Schindler J, Krance RA, Heslop HE, Spencer DM, Rooney CM, Brenner MK. Inducible apoptosis as a safety switch for adoptive cell therapy. N Engl J Med. 2011; 365:1673–1683. [PubMed: 22047558]
54. Wang X, Chang WC, Wong CW, Colcher D, Sherman M, Ostberg JR, Forman SJ, Riddell SR, Jensen MC. A transgene-encoded cell surface polypeptide for selection, in vivo tracking, and ablation of engineered cells. Blood. 2011; 118:1255–1263. [PubMed: 21653320]
55. Cooper LJ, Ausubel L, Gutierrez M, Stephan S, Shakeley R, Olivares S, Serrano LM, Burton L, Jensen MC, Forman SJ, DiGiusto DL. Manufacturing of gene-modified cytotoxic T lymphocytes for autologous cellular therapy for lymphoma. Cytotherapy. 2006; 8:105–117. [PubMed: 16698684]
56. Kloss CC, Condomines M, Cartellieri M, Bachmann M, Sadelain M. Combinatorial antigen recognition with balanced signaling promotes selective tumor eradication by engineered T cells. Nat Biotechnol. 2013; 31:71–75. [PubMed: 23242161]
57. Fedorov VD, Sadelain M, Kloss CC. Novel approaches to enhance the specificity and safety of engineered T cells. Cancer J. 2014; 20:160–165. [PubMed: 24667964]
58. Fedorov VD, Themeli M, Sadelain M. PD-1- and CTLA-4-based inhibitory chimeric antigen receptors (iCARs) divert off-target immunotherapy responses. Science translational medicine. 2013; 5:215ra172.
59. Beatty GL, Haas AR, Maus MV, Torigian DA, Soulen MC, Plesa G, Chew A, Zhao Y, Levine BL, Albelda SM, Kalos M, June CHH. Mesothelin-Specific Chimeric Antigen Receptor mRNA-Engineered T Cells Induce Antitumor Activity in Solid Malignancies. Cancer Immunol Res. 2014
60. Brentjens RJ, Santos E, Nikhamin Y, Yeh R, Matsushita M, La PK, Quintas-Cardama A, Larson SM, Sadelain M. Genetically targeted T cells eradicate systemic acute lymphoblastic leukemia xenografts. Clin Cancer Res. 2007; 13:5426–5435. [PubMed: 17855649]
61. Gade TP, Hassen W, Santos E, Gunset G, Saudemont A, Gong MC, Brentjens R, Zhong XS, Stephan M, Stefanski J, Lyddane C, Osborne JR, Buchanan IM, Hall SJ, Heston WD, Riviere I, Larson SM, Koutcher JA, Sadelain M. Targeted elimination of prostate cancer by genetically directed human T lymphocytes. Cancer Res. 2005; 65:9080–9088. [PubMed: 16204083]
62. Suzuki K, Servais EL, Rizk NP, Solomon SB, Sima CS, Park BJ, Kachala SS, Zlobinsky M, Rusch VW, Adusumilli PS. Palliation and pleurodesis in malignant pleural effusion: the role for tunneled pleural catheters. J Thorac Oncol. 2011; 6:762–767. [PubMed: 21325982]
63. van Herpen CM, van der Laak JA, de Vries IJ, van Krieken JH, de Wilde PC, Balvers MG, Adema GJ, De Mulder PH. Intratumoral recombinant human interleukin-12 administration in head and neck squamous cell carcinoma patients modifies locoregional lymph node architecture and induces natural killer cell infiltration in the primary tumor. Clin Cancer Res. 2005; 11:1899–1909. [PubMed: 15756016]
64. Carpenter SG, Carson J, Fong Y. Regional liver therapy using oncolytic virus to target hepatic colorectal metastases. Semin Oncol. 2010; 37:160–169. [PubMed: 20494708]
65. Maher J, Brentjens RJ, Gunset G, Riviere I, Sadelain M. Human T-lymphocyte cytotoxicity and proliferation directed by a single chimeric TCRzeta/CD28 receptor. Nat Biotechnol. 2002; 20:70–75. [PubMed: 11753365]
66. Hollyman D, Stefanski J, Przybylowski M, Bartido S, Borquez-Ojeda O, Taylor C, Yeh R, Capacio V, Olszewska M, Hosey J, Sadelain M, Brentjens RJ, Riviere I. Manufacturing validation of

biologically functional T cells targeted to CD19 antigen for autologous adoptive cell therapy. J Immunother. 2009; 32:169–180. [PubMed: 19238016]

67. McCoy JL, Herberman RB, Rosenberg EB, Donnelly FC, Levine PH, Alford C. 51 Chromium-release assay for cell-mediated cytotoxicity of human leukemia and lymphoid tissue-culture cells. National Cancer Institute monograph. 1973; 37:59–67. [PubMed: 4123455]
68. Adusumilli PS, Eisenberg DP, Stiles BM, Chung S, Chan MK, Rusch VW, Fong Y. Intraoperative localization of lymph node metastases with a replication-competent herpes simplex virus. J Thorac Cardiovasc Surg. 2006; 132:1179–1188. [PubMed: 17059941]
69. Servais EL, Colovos C, Kachala SS, Adusumilli PS. Pre-clinical mouse models of primary and metastatic pleural cancers of the lung and breast and the use of bioluminescent imaging to monitor pleural tumor burden. Curr Protoc Pharmacol. 2011; Chapter 14(Unit 14):21. [PubMed: 21898334]
70. Stiles BM, Adusumilli PS, Bhargava A, Stanziale SF, Kim TH, Chan MK, Huq R, Wong R, Rusch VW, Fong Y. Minimally invasive localization of oncolytic herpes simplex viral therapy of metastatic pleural cancer. Cancer Gene Ther. 2006; 13:53–64. [PubMed: 16037824]
71. Rabinovich BA, Ye Y, Etto T, Chen JQ, Levitsky HI, Overwijk WW, Cooper LJ, Gelovani J, Hwu P. Visualizing fewer than 10 mouse T cells with an enhanced firefly luciferase in immunocompetent mouse models of cancer. Proc Natl Acad Sci U S A. 2008; 105:14342–14346. [PubMed: 18794521]
72. Na IK, Markley JC, Tsai JJ, Yim NL, Beattie BJ, Klose AD, Holland AM, Ghosh A, Rao UK, Stephan MT, Serganova I, Santos EB, Brentjens RJ, Blasberg RG, Sadelain M, van den Brink MR. Concurrent visualization of trafficking, expansion, and activation of T lymphocytes and T-cell precursors in vivo. Blood. 2010; 116:e18-25. [PubMed: 20511541]

Author Manuscript

Author Manuscript

Author Manuscript

One Sentence Summary

Regional delivery of mesothelin-targeted CAR T cell therapy provides superior anti-tumor efficacy and long-term immunity against pleural malignancies compared to systemic administration.

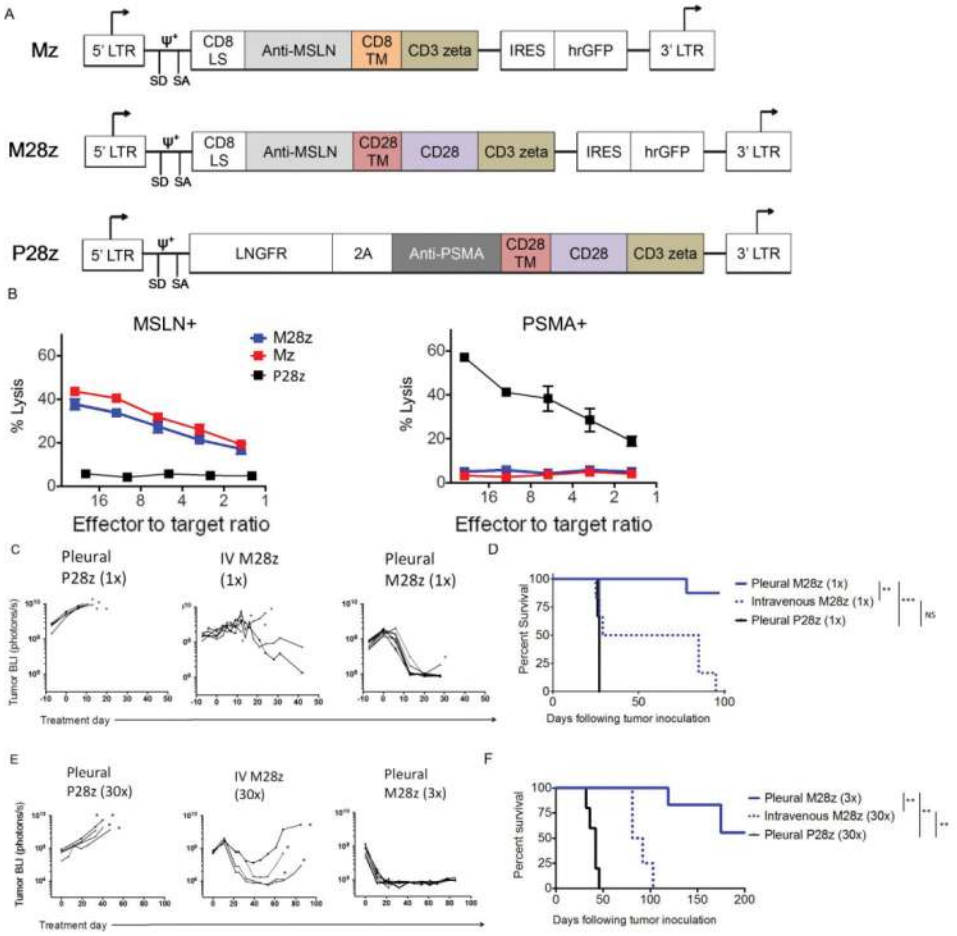

Fig. 1. Regional administration of MSLN CAR-transduced T cells results in superior antitumor efficacy

(A) MSLN-targeted constructs with CD3ζ endodomain alone (Mz) or with the CD28 costimulatory domain (M28z). A PSMA-directed CAR with CD28 costimulation (P28z) as well as PSMA+-expressing EL4 targets are included in experiments as negative controls. Antigen-specific effector function of MSLN-CAR–transduced T cells as shown by lysis of MSLN-expressing, but not PSMA-expressing, target cells measured by chromium-release assays. **(C and E)** Tumor BLI of NOD/SCID/γ_c^{null} mice bearing pleural tumor. Tumor-bearing mice were treated with either 1×10^5 (1×) or 3×10^6 (30×) M28z T cells intravenously (E:T, 1:3000 or 100, respectively), compared with 1×10^5 (1×) or 3×10^5 (3×) M28z T cells intrapleurally (E:T, 1:3000 or 1000, respectively). Death is depicted by an asterisk (*). **(D and F)** Kaplan-Meier survival analysis demonstrates superior efficacy with intrapleural administration (solid blue line), compared with intravenous administration (dashed blue line). Median survival was not reached for intrapleural administration of M28z; median survival for intravenous administration was 27 days (1×) and 86 days (30×). Control mice treated with pleural P28z (black line) had a median survival of 27 to 42 days (n=4-10 per group). Survival curves were analyzed with Log-rank test. $^{**}P < 0.01$; $^{***}P < 0.001$. Raw data and exact P values are provided in Supplementary Materials

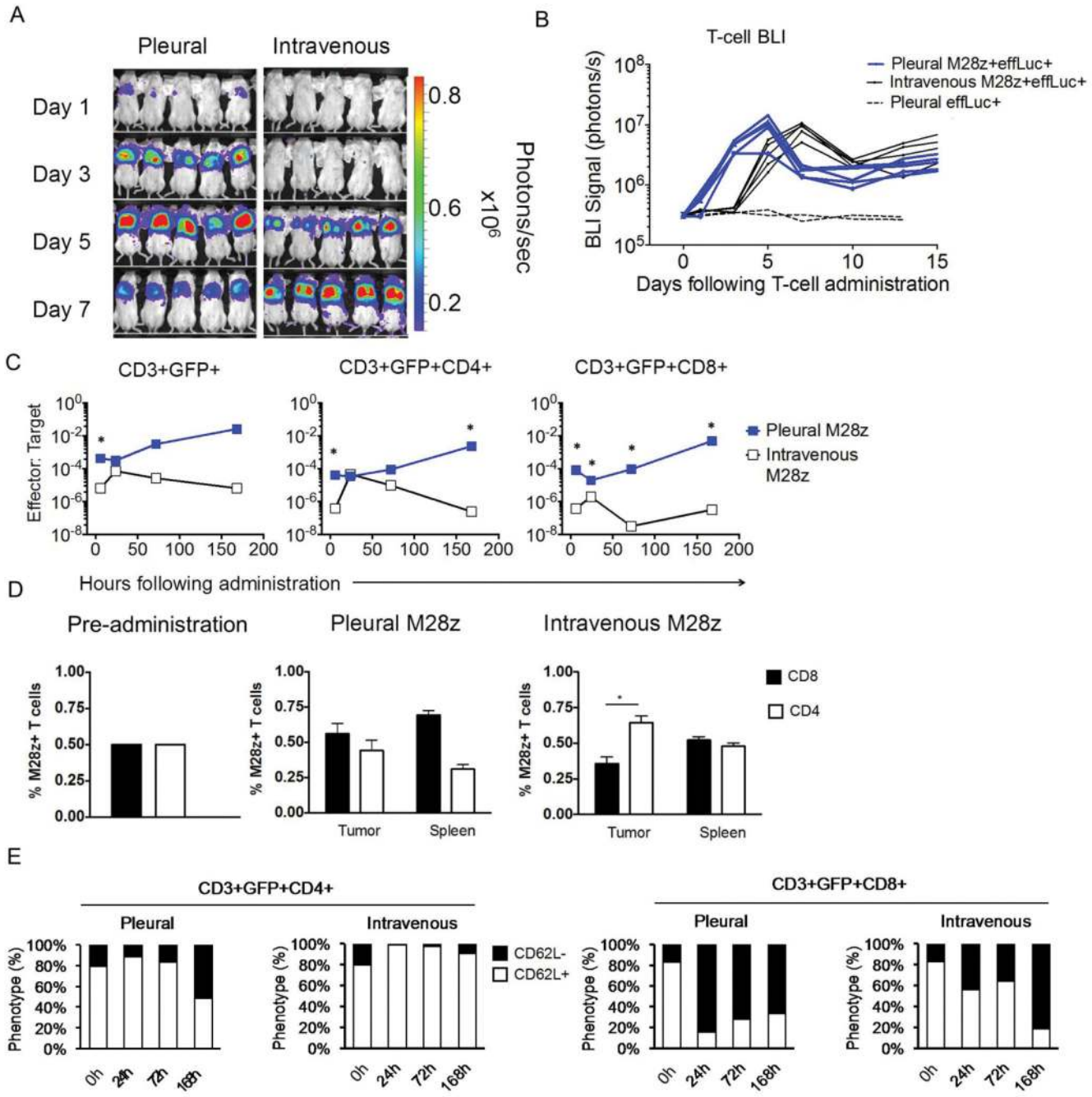

Fig. 2. Intrapleurally administered M28z+ T cells display early, robust proliferation of both CD4+ and CD8+ subsets

(A) Serial T-cell BLI in tumor-bearing mice. Intravenously administered M28z+ T cells display delayed but equivalent accumulation in the progressing pleural tumor. (**B**) Average effLuc-luciferase signal intensities from sequential T-cell BLI. Intrapleurally administered T cells (blue lines) display an earlier and sustained accumulation, with maximal T-cell signal at day 5. Intravenously administered T cells show delayed accumulation, with maximal signal at day 7. **(C)** E:T ratios reflect M28z T-cell accumulation in parallel with tumor

burden at 6 h and days 1, 3, and 7, confirming the findings of T-cell BLI. Intravenous administration shows delayed T-cell accumulation, lower E:T ratios, and decreased CD8+ T cell infiltration. (**D**) FACS analysis at day 7 displays an equal accumulation of CD4+ and CD8+ T-cell subsets within the tumor and spleen after intrapleural administration, compared with decreased tumor accumulation of CD8+ T cells and equal distribution of CD4+ and CD8+ T cells in the spleen after intravenous administration. (**E**) A decrease in CD62L expression was observed in both CD4+ and CD8+ T cells following intrapleural administration. Error bars represent ±SEM. *P <0.05, **P < 0.01, ***P <0.001 by Student's t test. Raw data and P values are provided in the Supplementary Materials.

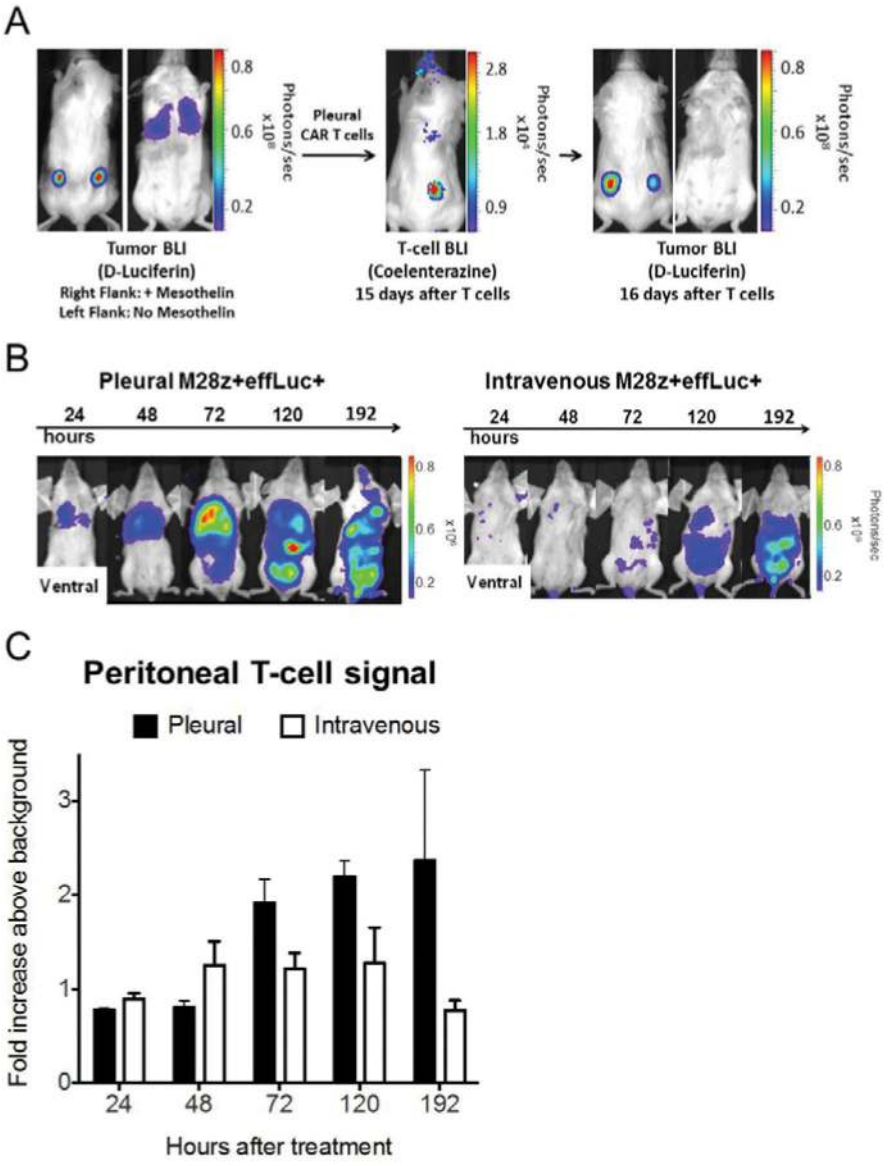

Fig. 3. Intrapleurally administered M28z+ T cells display efficient systemic trafficking and accumulation in extrapleural tumor in an antigen-specific manner

(A) Serial tumor and T-cell BLI with dual luciferase imaging, demonstrating systemic trafficking and extrapleural tumor accumulation. Mice with established ffluc+ MSLN+ tumor in the right flank and pleural cavity and MSLN- tumor in the left flank received Gaussia-luciferase+ M28z T cells intrapleurally. A representative mouse with tumor in the flanks and pleural cavity before T-cell administration (left). T-cell BLI 15 days after T-cell administration (center) demonstrates residual T cells in the pleural cavity and accumulation in the MSLN+ right-flank tumor (center). One day later, tumor BLI shows a reduced burden in the MSLN+ right-flank tumor, compared with the MSLN- left-flank tumor (right). **(B and C)** Intrapleurally administered M28z+ T cells show early and robust accumulation in MSLN + intraperitoneal tumor, compared with intravenously administered T cells. **(C)** Quantification of the fold increase in signal intensity of the peritoneal cavity in tumor-

bearing mice displays enhanced T-cell accumulation with intrapleural administration, compared with intravenous administration (n=3 per group, error bars represent ±SEM. Raw data and P values are provided in the Supplementary Materials).

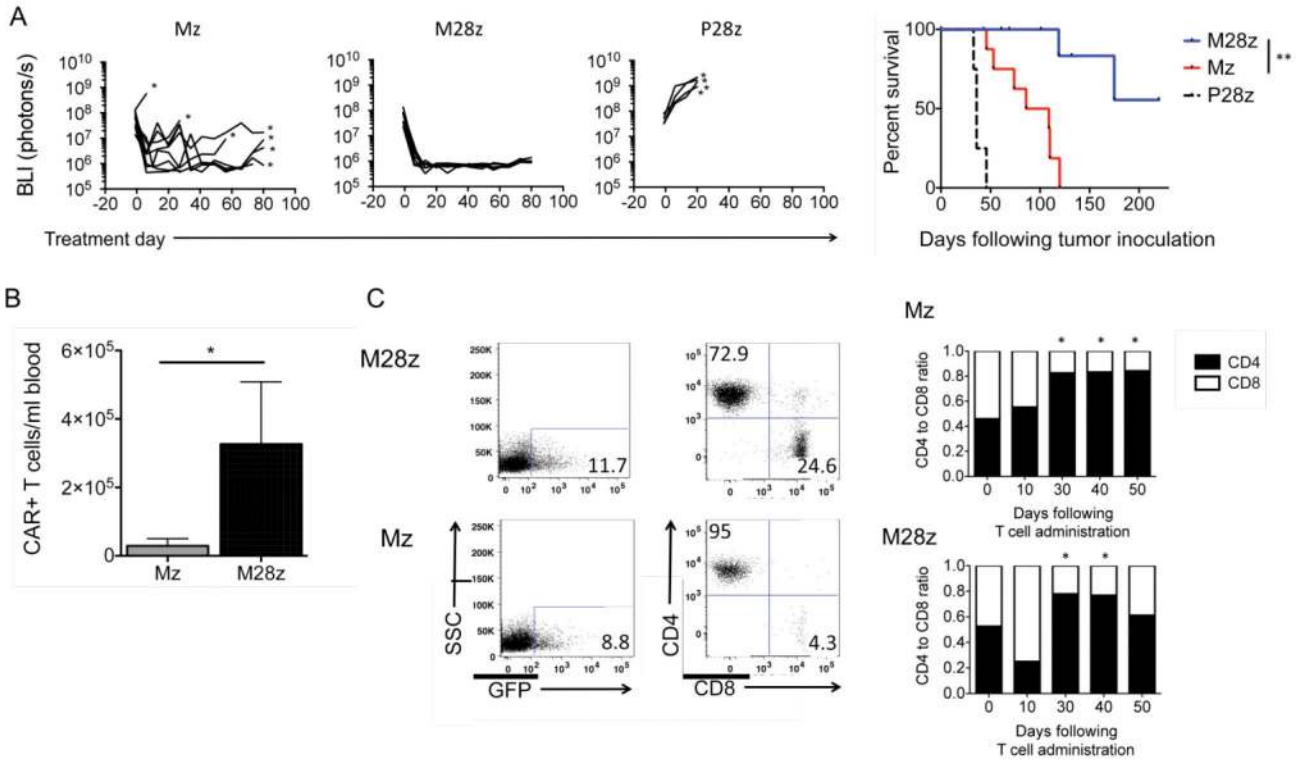

Fig. 4. Intrapleurally administered M28z T cells eradicate pleural tumor and establish long-term CD4+ predominant persistence

(A) CD28 costimulation facilitates tumor eradication following a single dose of T cells. In total, 1×10^5 CAR+ Mz, M28z, or P28z (negative control) T cells were intrapleurally administered into mice bearing established tumors. (Left) Tumor burden. (Right) Kaplan-Meier survival curve. Median survival of the Mz and M28z groups (at least 9 mice per group) was 63 days and median survival not reached, respectively. Survival curve was analyzed by log-rank test. **P<0.01. **(B)** CD28 costimulation enhances CAR+ T-cell persistence. Absolute CAR+ T-cell counts (per mL of peripheral blood) at 50 days after intrapleural administration of 3×10^6 CAR+ T cells. Error bars represent ±SEM, $*P < 0.05$ by Student's t test. **(C)** Persisting CAR+ T cells are predominantly CD4+. (Left) FACS analysis of peripheral blood in treated mice. (Right) CD4:CD8 ratios determined at successive time points following T-cell administration. The preinfusion CD4:CD8 ratio was approximately 0.5. Results shown are similar across a range of T-cell doses (3×10^6, 1×10^6, and 3×10^5 CAR+, n=3 mice at each time point). $*P<0.05$ by Student's test with Bonferroni correction for multiple comparisons comparing ratio at each time point to the preinfusion CD4:CD8 ratio. Raw data and P values are provided in the Supplementary Materials.

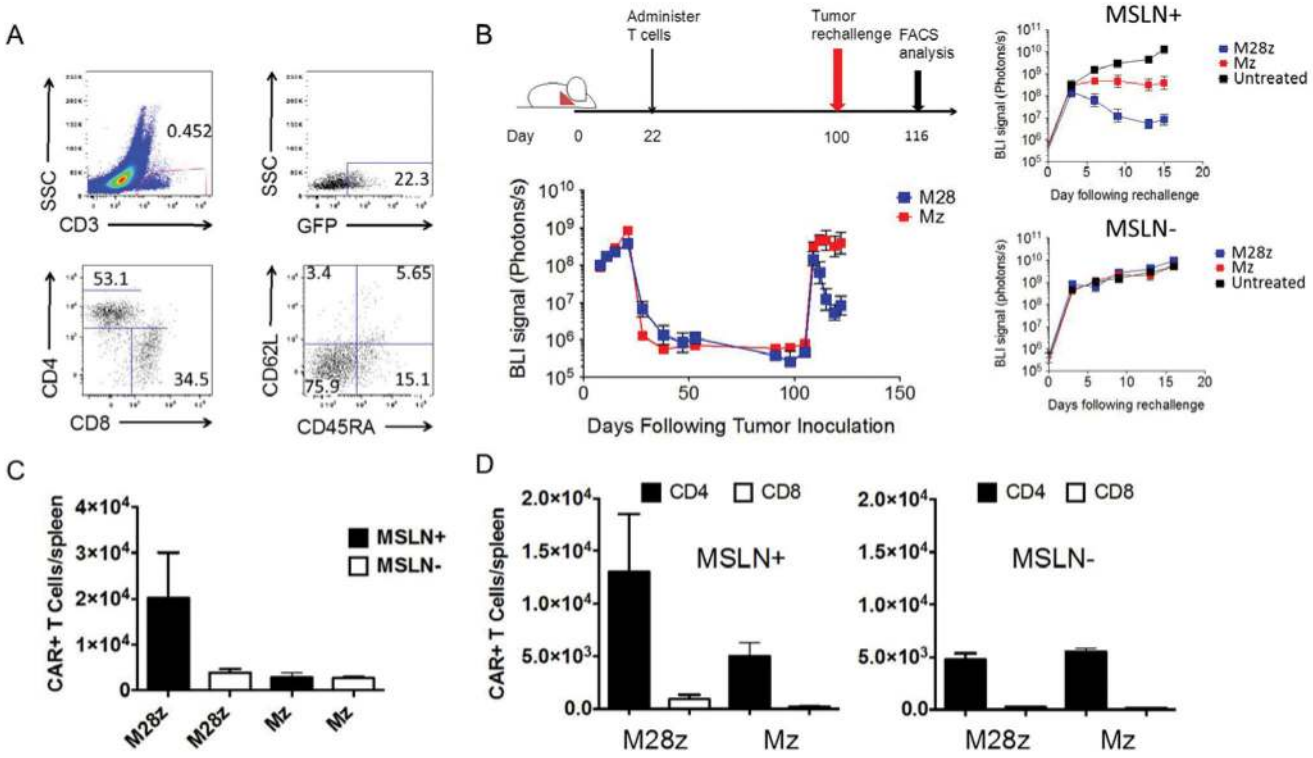

Fig. 5. Functional persistence of intrapleurally administered MSLN CAR T cells is predominantly mediated by CD4+ and is augmented by CD28 costimulation

(A) FACS analysis of splenic single-cell suspension prepared from mice (n=3) sacrificed 202 days after tumor eradication, following a single dose of 3×10^5 M28z T cells administered intrapleurally. CD3+GFP+M28z T cells show a predominance of effector memory CD4+ T cells. **(B)** Tumor BLI of mice rechallenged with MSLN+ and MSLN- tumor. Eighty-seven days after pleural tumor eradication, following administration of a single dose of 3×10^5 M28z or Mz T cells, 1×10^6 MSLN+ or MSLN- tumor cells were injected into the peritoneal cavity. Following tumor rechallenge, Mz T cells prevent tumor growth, whereas M28z T cells promote tumor regression. **(C and D)** Absolute M28z or Mz T-cell numbers in the spleen after tumor rechallenge with either MSLN+ (n=6) or MSLN- (n=6) tumor; mice were sacrificed 16 days after tumor rechallenge. Only the M28z T-cell–treated mice rechallenged with MSLN+ tumor show a robust accumulation of CAR+ T cells in the spleen, the majority of which are CD4+ T cells. Error bars represent ±SEM, raw data and P values are provided in the Supplementary Materials.

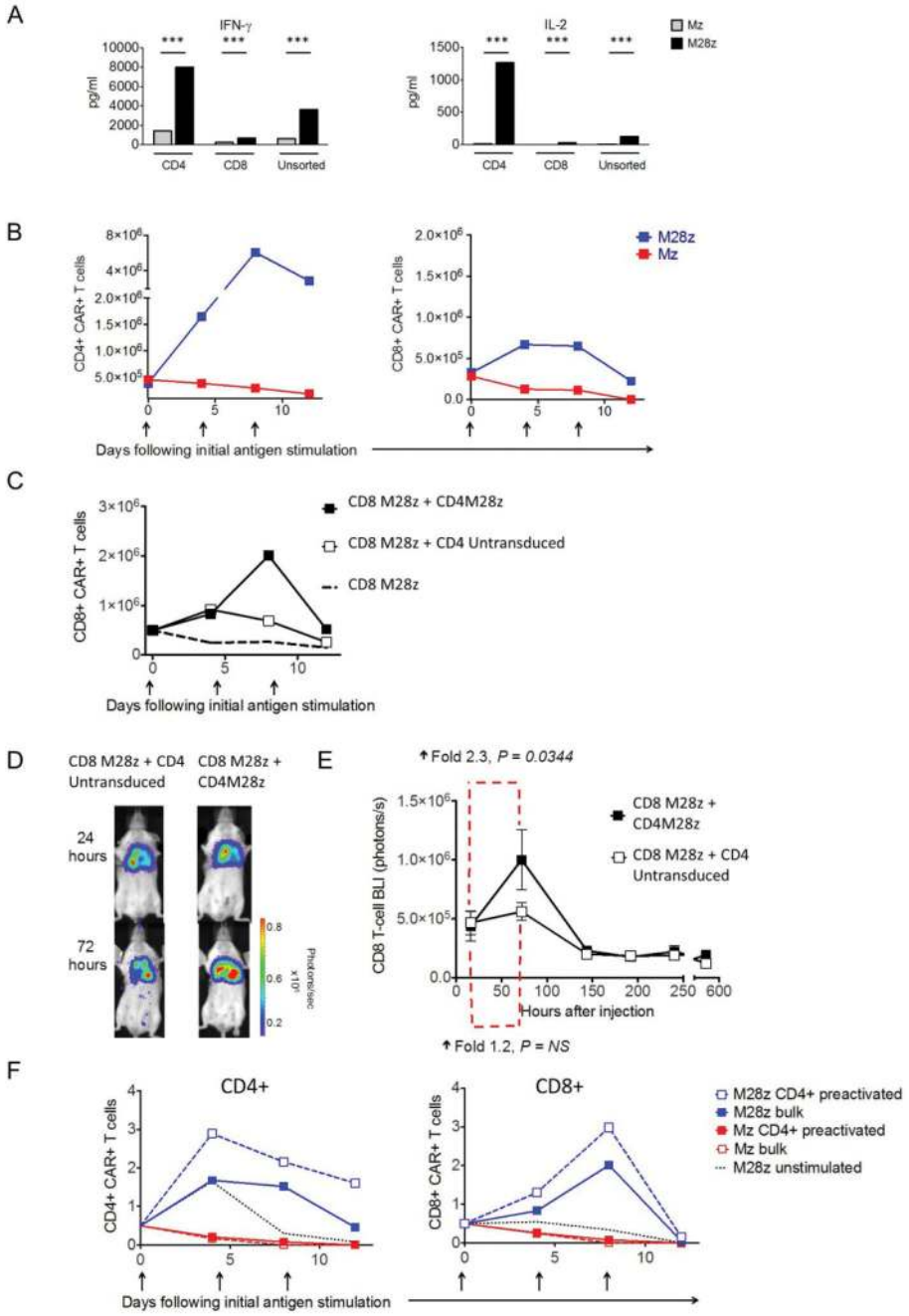

Fig. 6. CD4+ M28z T cells augment CD8+ accumulation that is enhanced with preactivation

(A–C) Unsorted M28z and Mz or bead-sorted CD4+ and CD8+ T cells were assayed. M28z CD4+ T cells show **(A)** higher cytokine secretion (from 4- to 14-fold; ***P<0.001 by Student's t test) and **(B)** profound T-cell expansion without exogenous IL-2. **(C)** CD4+ M28z activation facilitates robust CD8+ M28z T-cell accumulation upon repeated antigen stimulation *in vitro*. **(D)** Antigen-activated CD4+ M28z activation facilitates robust CD8+ M28z T-cell accumulation *in vivo*. Isolated CD8+ effLuc M28z T cells were intrapleurally administered to MSLN+ pleural tumor–bearing mice with either CD4+ M28z (n=6) or

CD4+ control–transduced T cells (n=6) and were serially imaged. One representative mouse (n=6 per group; left) displays increased CD8+ M28z T-cell accumulation in the presence of CD4+ M28z. **(E)** The average accumulation of CD8+ CAR+ T cells was calculated at the indicated intervals (P values as shown calculating fold increase from 16 to 72 hours, n=6 per group). **(F)** Preactivation of M28z CD4+ enhances CD8+ proliferation, compared with simultaneous activation of CD4+. Bead-sorted CD8+ Mz or M28z T cells were cocultured with either corresponding Mz or M28z CD4+ or preactivated CD4+ T cells (activated on MSLN+ tumor cells 24 h before the assay). Preactivation of M28z CD4+ enhances the accumulation of CD8+ to a greater degree than does CD8+ and CD4+ concurrent stimulation.

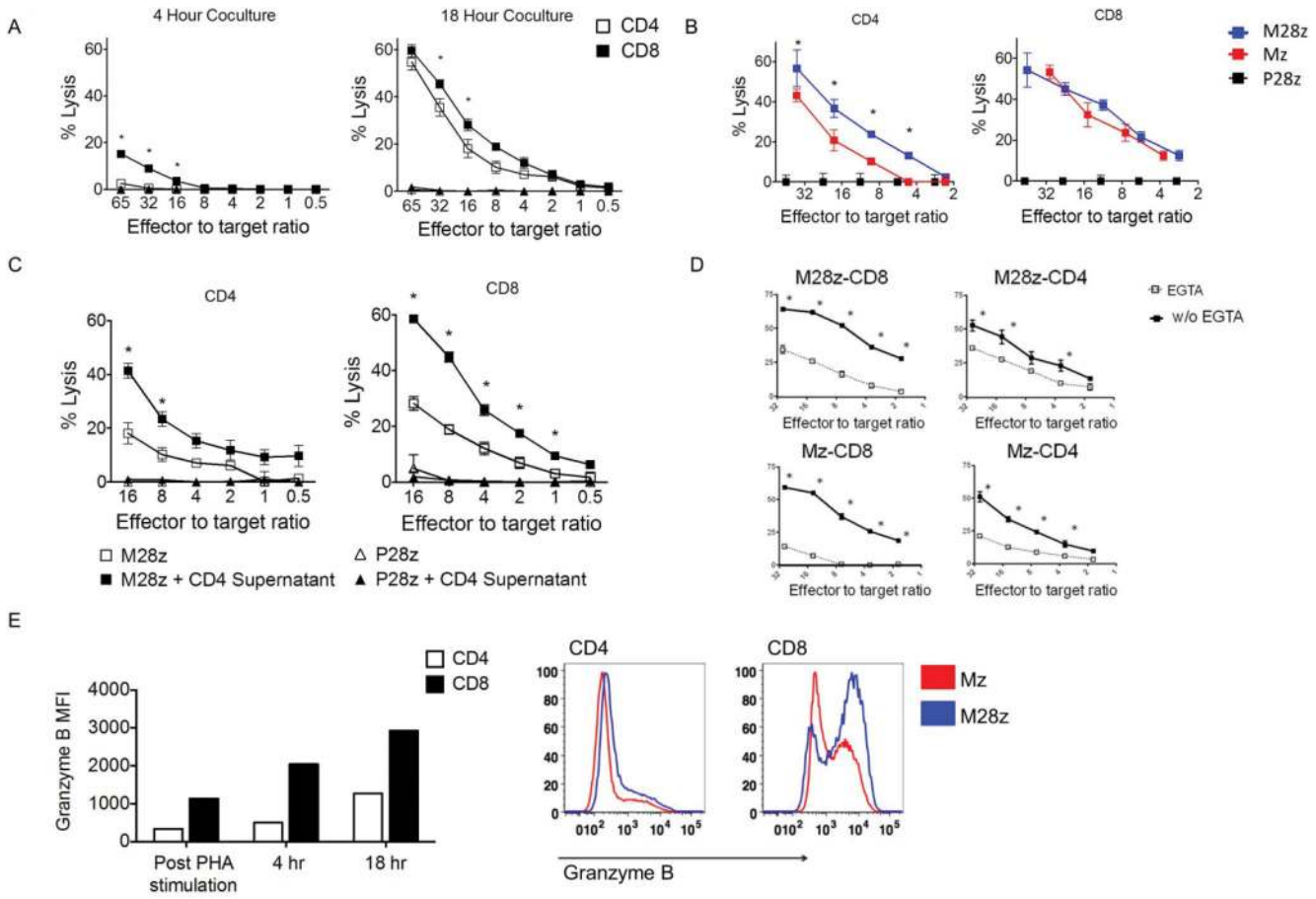

Fig. 7. CD4+ MSLN CAR+ T cells demonstrate efficient cytolytic function that is granzyme/perforin dependent

(A) CD4+ M28z T cells show a delayed but similar cytotoxicity as CD8+ M28z T cells. **(B)** CD28 costimulation enhances CD4+-mediated cytotoxicity. **(C)** Cytokine-rich supernatants obtained from stimulated CD4+ M28z CAR+ T cells enhance cytotoxicity of both CD8M28z and CD4M28z T cells. **(D)** CAR T-cell lytic function is dependent on release of cytotoxic granules. Bulk, CD4, or CD8 M28z and Mz T cells were cocultured for 18 h in the presence or absence of the chelating agent **ethylene glycol tetraacetic acid** (EGTA). **(A–D)** Cytotoxicity of bead-purified CD4+ or CD8+ Mz and M28z T cells. (**E**, left) CD4+ CAR T cells express granzyme B, but with delayed kinetics, compared with CD8+ CAR T cells. Intracellular FACS analysis for granzymes B was performed on resting PBMCs, PHA-stimulated blasts, and M28z, Mz, and P28z T cells stimulated with MSLN+ for 4 or 18 h.(E, right) CD28 costimulation enhances granzyme B expression. Histograms show expression at 18 h after MSLN+ stimulation. Error bars represent ±SEM, $*P < 0.05$ by Student's t test. Raw data and P values are provided in the Supplementary Materials.

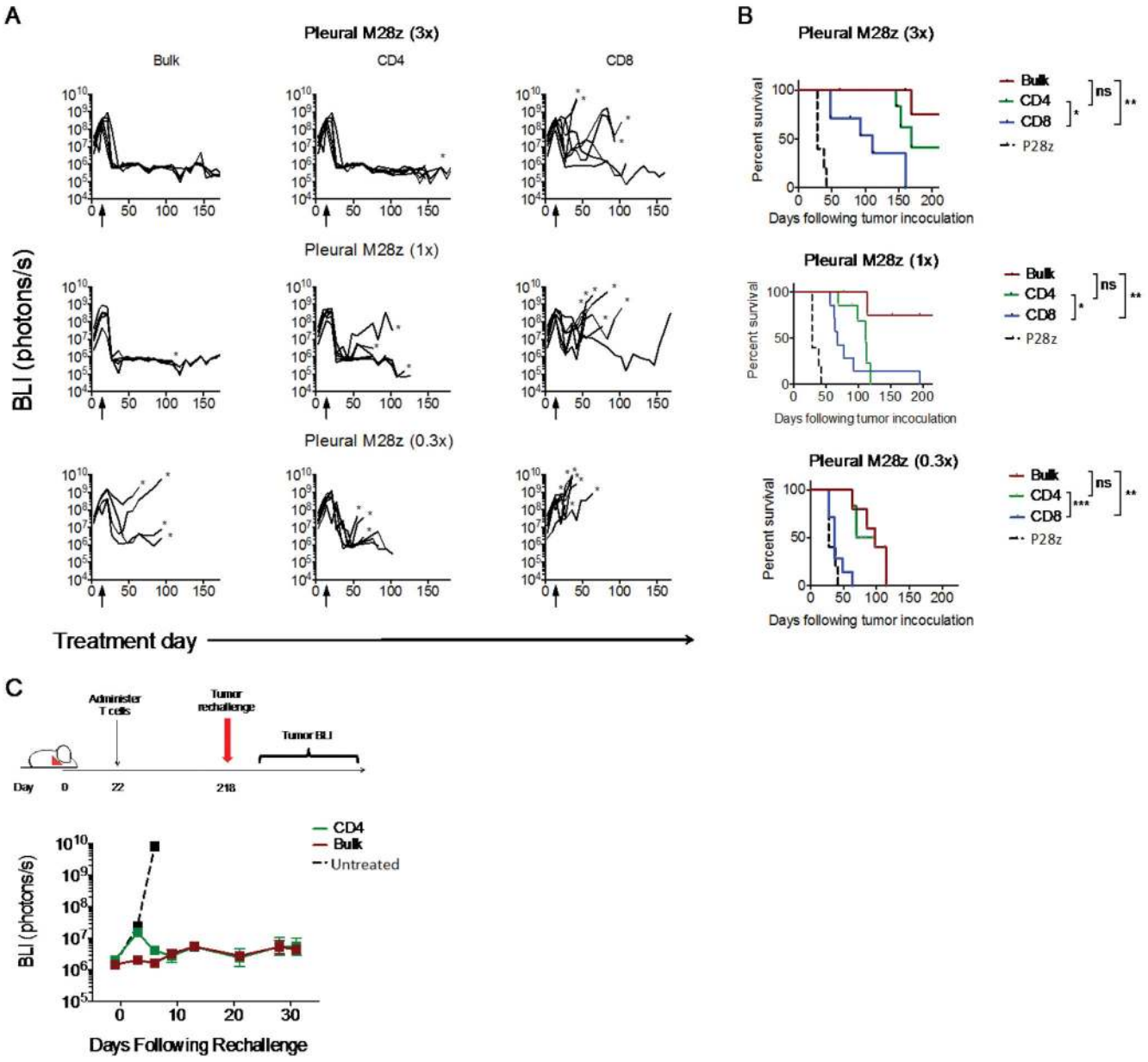

Fig. 8. Intrapleurally administered CD4+ M28z CAR T cells are efficacious when administered alone *in vivo*; mediate enhanced efficacy, compared with CD8+ M28z T cells; and establish long-term functional persistence

(A) BLI tracking the progression of tumor burden. Eighteen days after tumor injection, mice received either 3×10^5 (3x), 1×10^5 (1x), or 3×10^4 (0.3x) CAR+ T cells of bulk M28z (n=5), bead-sorted CD4+, CD8+ M28z (n=7), or P28z (n=4). **(B)** Kaplan-Meier survival curves. At all doses, CD4+ M28z CAR+ T cells were efficacious, compared with CD8+ CAR+ T cells. The antitumor efficacy of CD4+ CAR+ T cells was comparable to that of unsorted CAR+ T cells. $*P < 0.05$; $**P < 0.01$; $***P < 0.001$ by Student's t test. Raw data and P values are provided in the Supplementary Materials. **(C)** Tumor BLI of mice rechallenged with tumor. At 196 days after intrapleural administration of a single dose of 3×10^5 (3x) unsorted (bulk)

M28z or CD4+-sorted M28z T cells, 1×10^6 MSLN+ tumor cells were injected into the peritoneal cavity. Persisting CD4+ M28z T cells prevented tumor growth.